Journal Name

Cite this: DOI: 10.1039/c0xx00000x

www.rsc.org/xxxxxx

ARTICLE TYPE

Symmetric Naphthalenediimidequaterthiophenes for Electropolymerized Electrochromic Thin Films

V. Figà,[a] C. Chiappara,[a] F. Ferrante,[a] M. P. Casaletto,[b] F. Principato,[a] S. Cataldo,[a] Z. Chen,[c] H. Usta,[c] A. Facchetti*[c,d] and B. Pignataro*[a]

[a] Dipartimento di Fisica e Chimica, Università di Palermo, V.le delle Scienze ed. 17, 90128, Palermo, Italy Fax: 0039-590015; Tel: 0039-09123897983;

[b] Istituto per lo Studio dei Materiali Nanostrutturati (ISMN), Consiglio Nazionale delle Ricerche (CNR), via Ugo La Malfa, 153, 90146 Palermo, Italy;

[c] Polyera Corporation, 8045 Lamon Avenue, Skokie, IL 60077 (USA).

[d] Center of Excellence for Advanced Materials Research, King Abdulaziz University , Jeddah 21589, Saudi Arabia.

*Correspondence to: bruno.pignataro@unipa.it; afacchetti@polyera.com

Electronic Supporting Information

Contents

---

1. Synthesis of Symmetric NDIT Systems and characterization

.

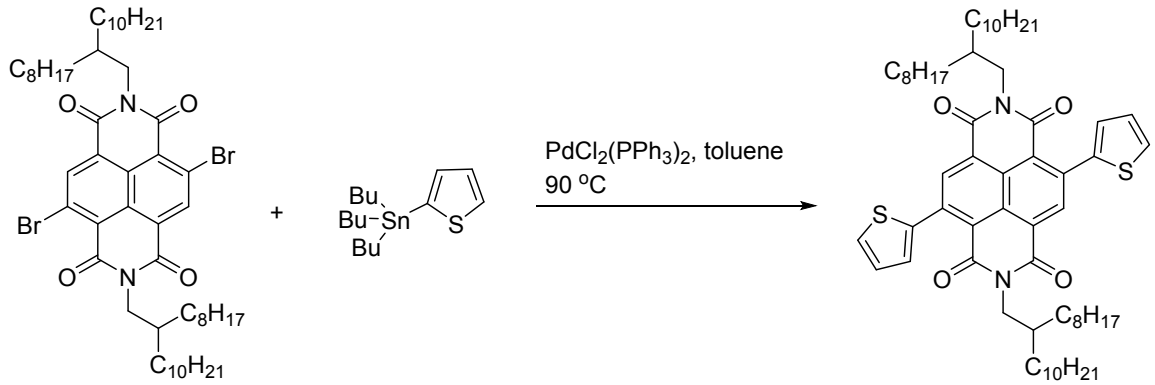

Scheme S1- Synthesis of s-NDI2ODT2

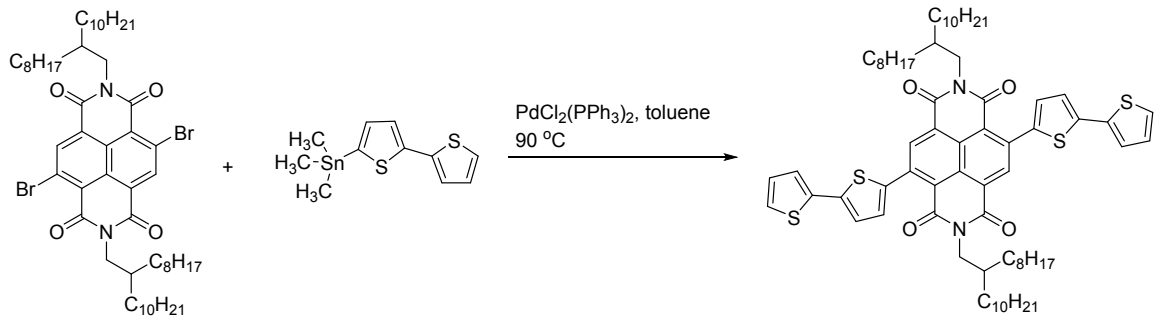

Scheme S2- Synthesis of s-NDI2ODT4

From optical absorption spectroscopy in acetonitrile:dichloromethane solution (2:3; v:v), the maximum absorption for s-NDI2ODT2 and s-NDI2ODT4 are located at 250 nm and 300 nm, respectively as shown in Figure S1

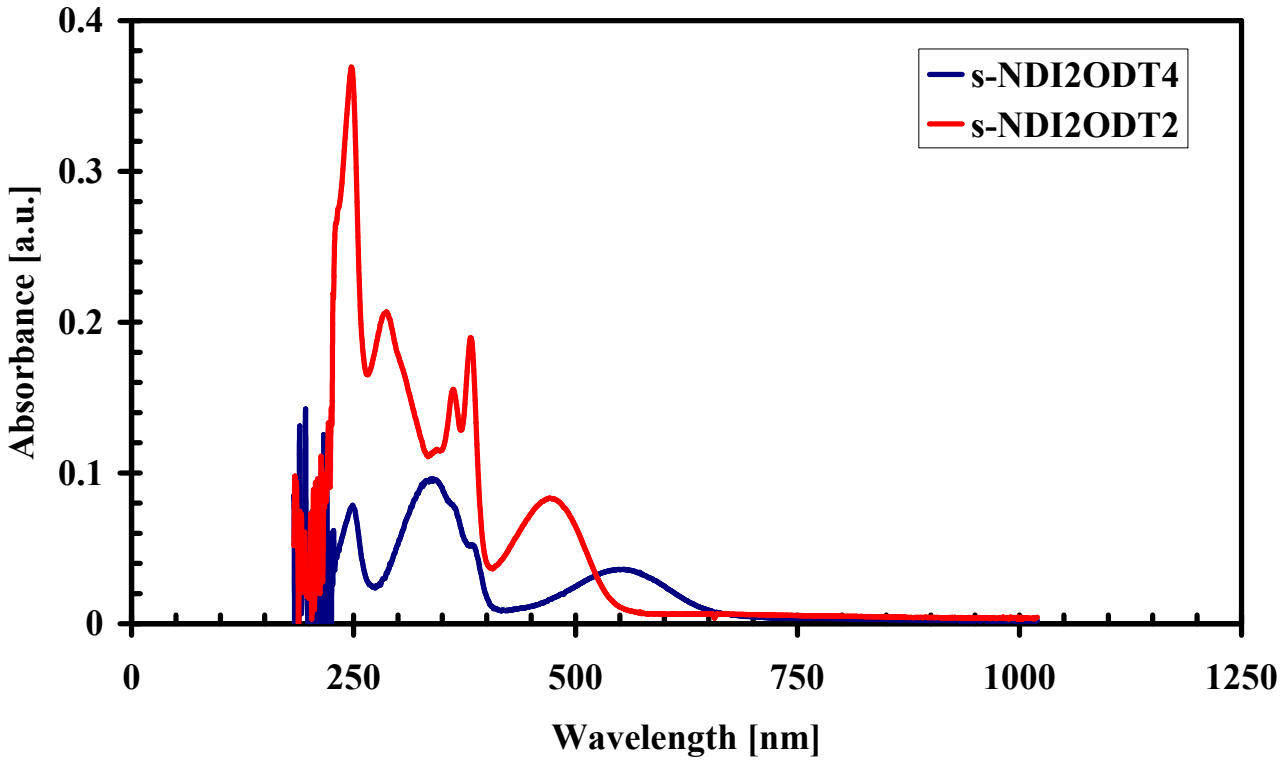

Figure S1 – Absorption spectra of s-NDI2ODT2 and s-NDI2ODT4 recorded in CH2Cl2:CH3CN (3:2; v:v)

Cyclic voltammetry (CV) measurements carried out in acetonitrile:dichloromethane solution (2:3; v:v) containing 10^{-2} M of $LiClO_4$ and 10^{-4} M of the monomers indicate oxidation onset potentials located at +1.6V and +1.15V for s-NDI2ODT2 and s-NDI2ODT4, respectively and oxidation peaks located at +1.8V and +1.24 V, for s-NDI2ODT2 and s-NDI2ODT4 respectively.

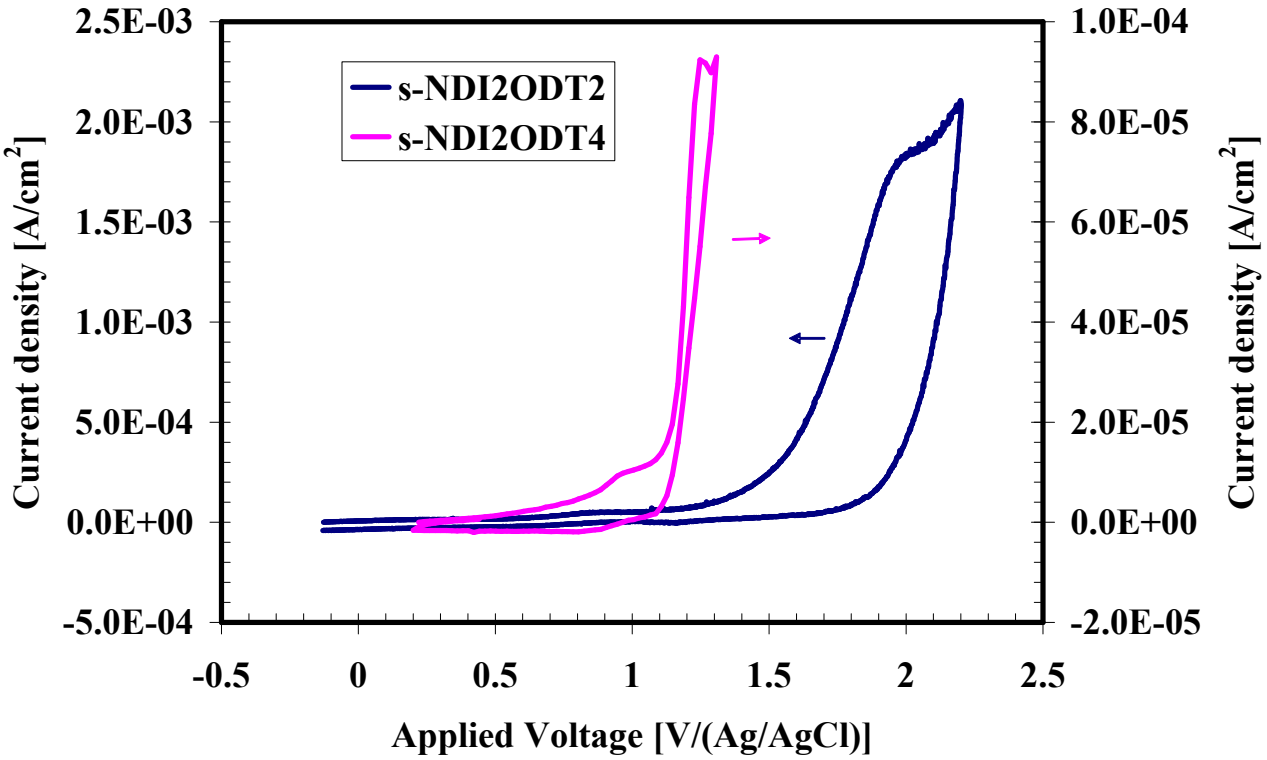

Figure S2 – Cyclic voltammograms of s-NDI2ODT2 and s-NDI2ODT4 recorded in CH2Cl2:CH3CN (3:2; v:v) and 0.1M LiClO4. Scan rate: 50 mVs^{-1}

2. Oxidation of NDI2ODT4 and EDOT

Before electropolymerization, preliminary experiments have been performed in order to know the oxidation potentials along with the co-polymerization availability of the NDI2ODT4 and EDOT monomers. For this purpose, the linear sweep voltammetry (LSV) technique has been employed. The electrolytic solutions have been made of CH_2Cl_2:CH_3CN (2:3; v:v%) containing 10^{-4}M NDI2ODT4 and 10^{-4}M EDOT, respectively. A Metrohm Autolab PGSTAT 128N Potentiostat/Galvanostat has been used for varying linearly the applied potential from the open circuit value. The potential scan rate has been 50 mVs^{-1}. The current vs potential plots, displayed in Figure S 3, have underlined that oxidation processes have taken place for both the monomer systems at potentials higher than 1.1 V vs Ag/AgCl. The proximity of NDI2ODT4 and EDOT oxidation potential onsets suggests the possibility of their copolymerization.

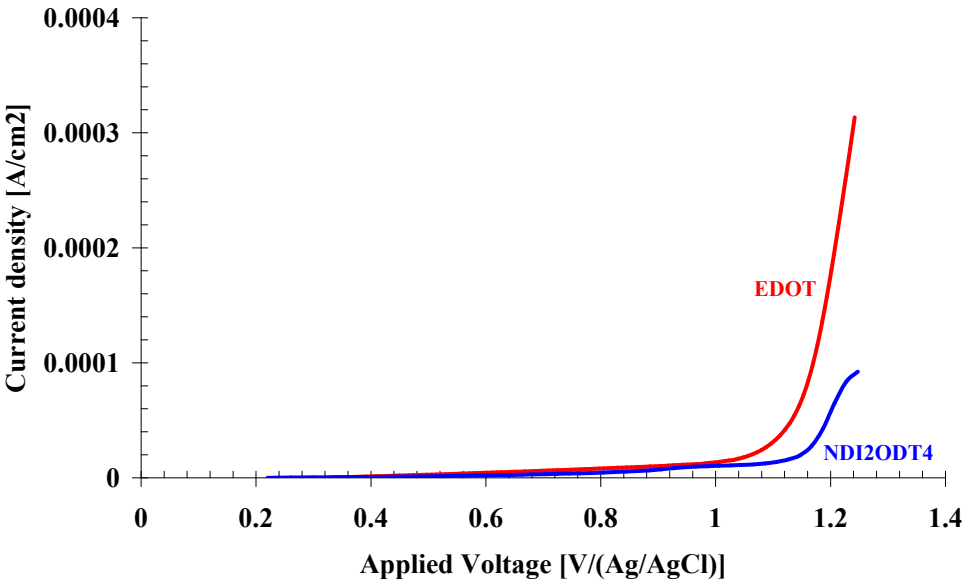

Figure S3 – Linear sweep voltammetries of 10^{-4} M NDI2ODT4 and 10^{-4} M EDOT, recorded in CH_2Cl_2:CH_3CN (3:2; v:v) containing 10^{-2} M $LiClO_4$ at 50 mVs^{-1}.

3. Cyclic Voltammetry during Electropolymerization

The deposition curve of homopolymers (figs. S4 a,b) are different from that of NDI2ODT4:EDOT 10:1 copolymers (Figure S 4c) as well as from that of the other copolymer systems with increasing EDOT amount (data not shown). This corroborates the copolymerization process under the potential scan. In particular in the PNDI2ODT4 system an oxidation onset at 1.17 V and an oxidation peak at 1.23 V are observed (potentials referred to Ag/AgCl 3.5 M), whereas in EDOT rich systems different curve shapes along with different open circuit voltages and no oxidation peaks are found.

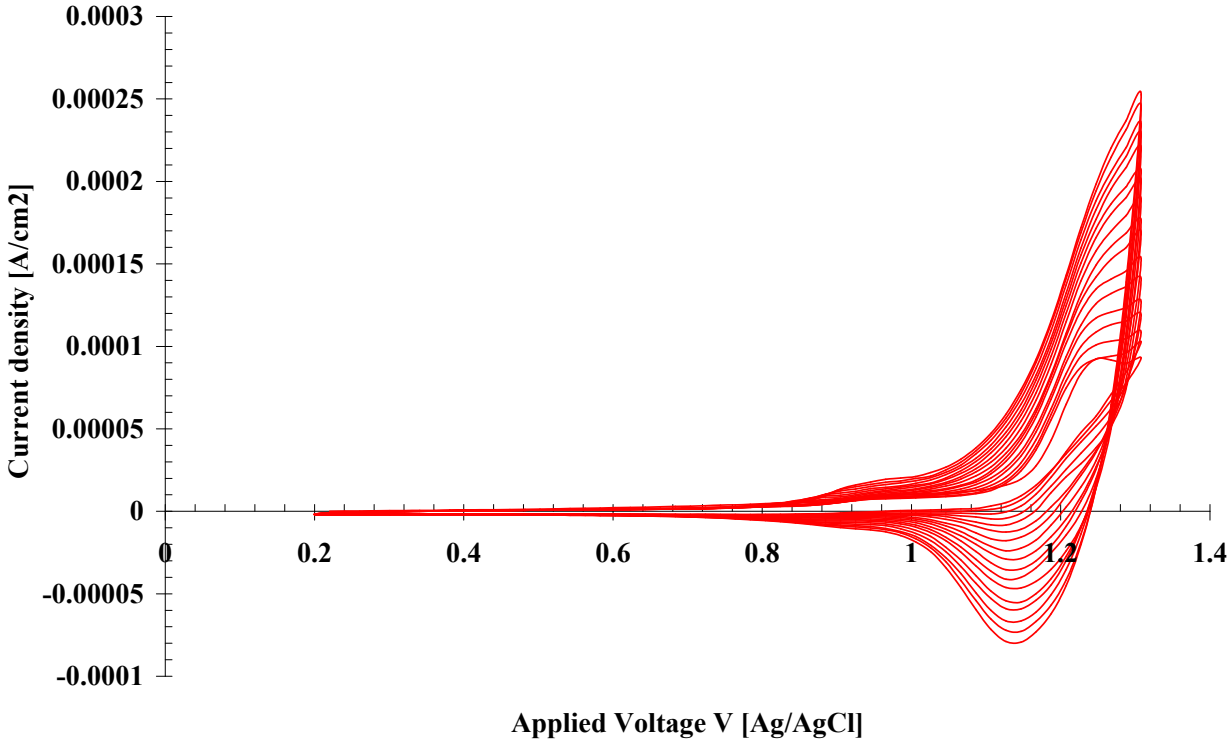
0.0003
0.00025
0.0002
0.00015
0.0001
0.00005
0
-0.00005
-0.0001
Current density [A/cm2]
0
0.2
0.4
0.6
0.8
1
1.2
1.4
Applied Voltage V [Ag/AgCl]

a)

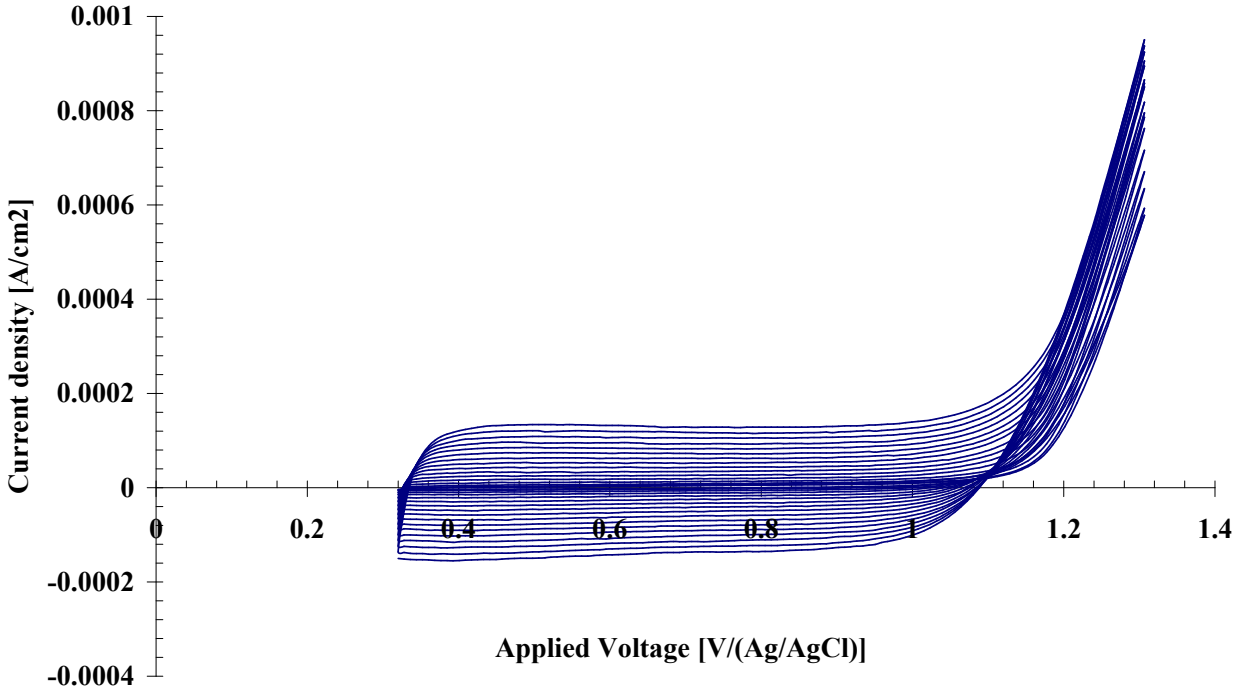
0.001
0.0008
0.0006
0.0004
0.0002
0
-0.0002
-0.0004
Current density [A/cm2]
0
0.2
0.4
0.6
0.8
1
1.2
1.4
Applied Voltage [V/(Ag/AgCl)]

b)

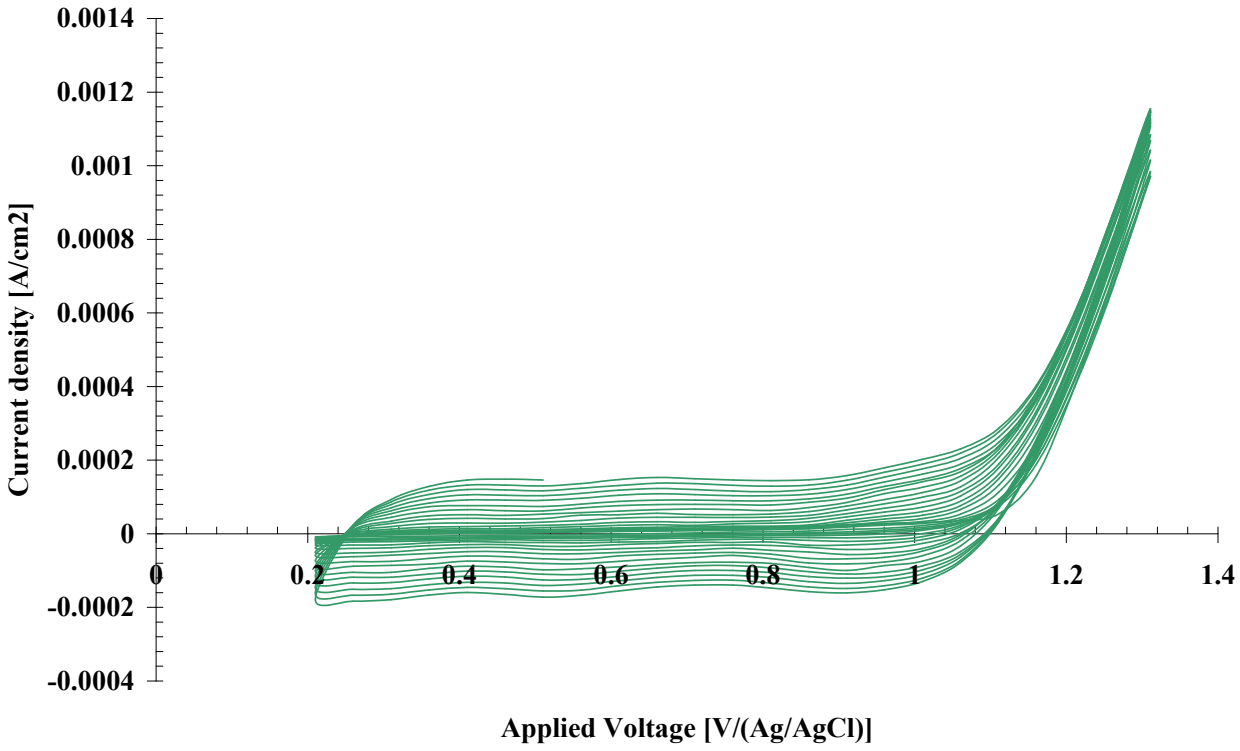

c)

Figure S4 – Electrodeposition curves of: a) PNDI2ODT4, b) PEDOT, c) copol **[1]**.

4. Polymerization Kinetics

Figure S5 shows the dependence of the peak current density from the potential scan rate in the range 10 - 150 mV/s. Note a shift of the anodic peak towards higher potential values.

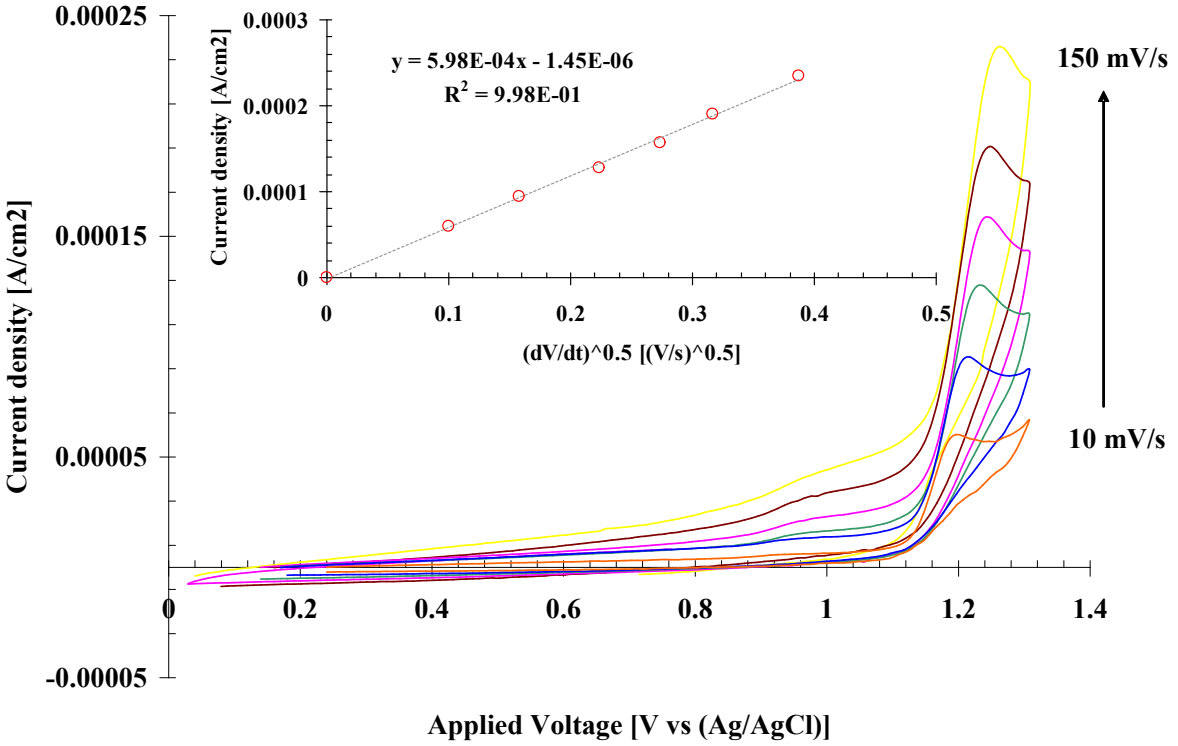

Figure S5 – Cyclic voltammetry of s-NDI2ODT4 at different scan rates in CH_2Cl_2:CH_3CN (3:2; v:v) containing 10^{-2} M $LiClO_4$.

By plotting the current density of the anodic peaks against the square root of the potential scan rate, a linear dependence has been found suggesting that the NDI2ODT4 electrochemical polymerization is controlled by a mass transport process.

By considering the Randles-Sevcik equation:

$$I_p = (2.69 \times 10^5) n^{\frac{3}{2}} A D^{\frac{1}{2}} c v^{\frac{1}{2}}$$

where I_p is the current peak, n is the number of electrons involved in the reaction, A is the electrode surface, D is the diffusion coefficient of the electroactive species, c is the monomer concentration and v is the potential scan rate, it is possible to calculate the diffusion coefficient from the slope of the best fitting straight line. For a monomer concentration of 10^{-4} molL^{-1} in a mixture of CH_3CN:CH_2Cl_2 (2:3; % vol), a diffusion coefficient of 4.2 E-05 cm^{2}s^{-1} has been calculated by

imposing n=2.25 [5] and A=0.07 cm^2.

5. DFT Calculations

The different phase of HOMO and LUMO in one of the linking points should be an evidence of the direct band gap nature of the corresponding (EDOT:NDI2ODT4:EDOT)$_n$ polymeric system (see Ref. [**6**]). In particular, the relative phases (– blue, – blue) and (+ red, – blue) of HOMO and LUMO at the linking points should indicate a direct band gap behaviour in a point of the reciprocal space having simmetry other than Γ. It is to note that we assumed as valid the reasoning of Seo et al.[**6**], which rigorously applies to extended conjugated π systems.

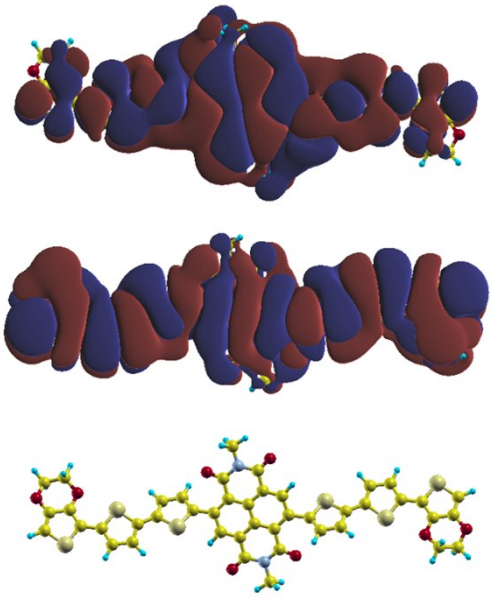

Figure S6 - HOMO (middle) and LUMO (top) representations of the EDOT:NDI2ODT4:EDOT molecular species (bottom). A very small MO isovalue has been chosen in order to visualize the small contribution of π orbitals of thiophene moieties near the linking points in the LUMO.

Table S1. The characteristics of the first three singlet-singlet adiabatic transitions (energy in eV / oscillator strength and character) in molecular systems formed by NDI2ODT4 and EDOT, calculated by means of the TD-CAM-B3LYP/cc-pvdz approach.

	$S_0 \rightarrow S_1$	$S_0 \rightarrow S_2$	$S_0 \rightarrow S_3$
$(NDI2ODT4)_2$	2.472 / 2.25 CT	2.603 / 0.00	2.894 / 0.02
NDI2ODT4-EDOT- NDI2ODT4	2.385 / 2.38 CT	2.508 / 0.06	2.863 / 0.04
NDI2ODT4-$(EDOT)_4$- NDI2ODT4	2.225 / 2.99 CT	2.306 / 0.04	2,699 / 1.51 $\pi \rightarrow \pi^*$
$(EDOT)_8$	2.588 / 3.11 $\pi \rightarrow \pi^*$	3.141 / 0.00	3.812 / 0.00
$(EDOT)_{12}$	2.432 / 4.98 $\pi \rightarrow \pi^*$	2.779 / 0.00	3.140 / 0.4
$(EDOT)_{16}$	2.365 / 6.85 $\pi \rightarrow \pi^*$	2.604 / 0.00	2.871 / 0.5
$(EDOT)_3$- NDI2ODT4-$(EDOT)_3$	2.212 / 2.10 CT	2.440 / 0.01	2.821 / 2.00 $\pi \rightarrow \pi^*$
$(EDOT)_4$- NDI2ODT4-$(EDOT)_4$	2.197 / 2.29 CT	2.407 / 0.00	2.810 / 3.44 $\pi \rightarrow \pi^*$
$(EDOT)_5$- NDI2ODT4-$(EDOT)_5$	2.175 / 2.63 CT	2.368 / 0.00	2.703 / 4.03 $\pi \rightarrow \pi^*$
$(EDOT)_6$- NDI2ODT4-$(EDOT)_6$	2.165 / 2.93 CT	2.344 / 0.00	2.625 / 4.56 $\pi \rightarrow \pi^*$
$(EDOT)_7$- NDI2ODT4-$(EDOT)_7$	2.156 / 3.24 CT	2.326 / 0.00	2.566 / 5.21 $\pi \rightarrow \pi^*$
$(EDOT)_8$- NDI2ODT4-$(EDOT)_8$	2.151 / 3.52 CT	2.315 / 0.00	2.520 / 5.84 $\pi \rightarrow \pi^*$

The characters of the transitions reported in Table 1 are labeled CT (charge transfer) or $\pi \rightarrow \pi^*$ according to the nature of molecular orbitals whit major weights in the description of the electronic states involved.

It can be noted, by comparing $(EDOT)_n$ to $(EDOT)_{n/2}$-NDI2ODT4-$(EDOT)_{n/2}$ data, how the inclusion of one NDI2ODT4 unit between a $(EDOT)_n$ chain causes the appearance of a low energy CT transition and a shift of the $\pi \rightarrow \pi^*$ transition to higher energy (due to the interrupted conjugation). The $S_0 \rightarrow S_1$ transition is always more intense than the $S_0 \rightarrow S_3$ one, and in between the $S_0 \rightarrow S_2$ transition is essentially prohibited. Its nature cannot be clearly labeled, since a number of differently localized MO are involved.

6. Optical band gaps

Thin films optical band gaps have been calculated by using the following equation [7]:

$$\alpha = \frac{A\left(h\nu - E_g\right)^n}{h\nu} \qquad (1)$$

where α is the absorption coefficient of the film, A is a constant, $h\nu$ is the photon energy and E_g is the optical band gap. n is a coefficient which assumes different values according to the permitted transitions; n= 2 and n=½ for indirect and direct optical transitions, respectively.

Figure S7a shows the optical spectrum of PNDI2ODT4 and its elaboration (see insets) under the

hypothesis of direct optical transitions.

By fitting the straight line portion at lower energies, a band gap values of 1.71eV have been calculated.

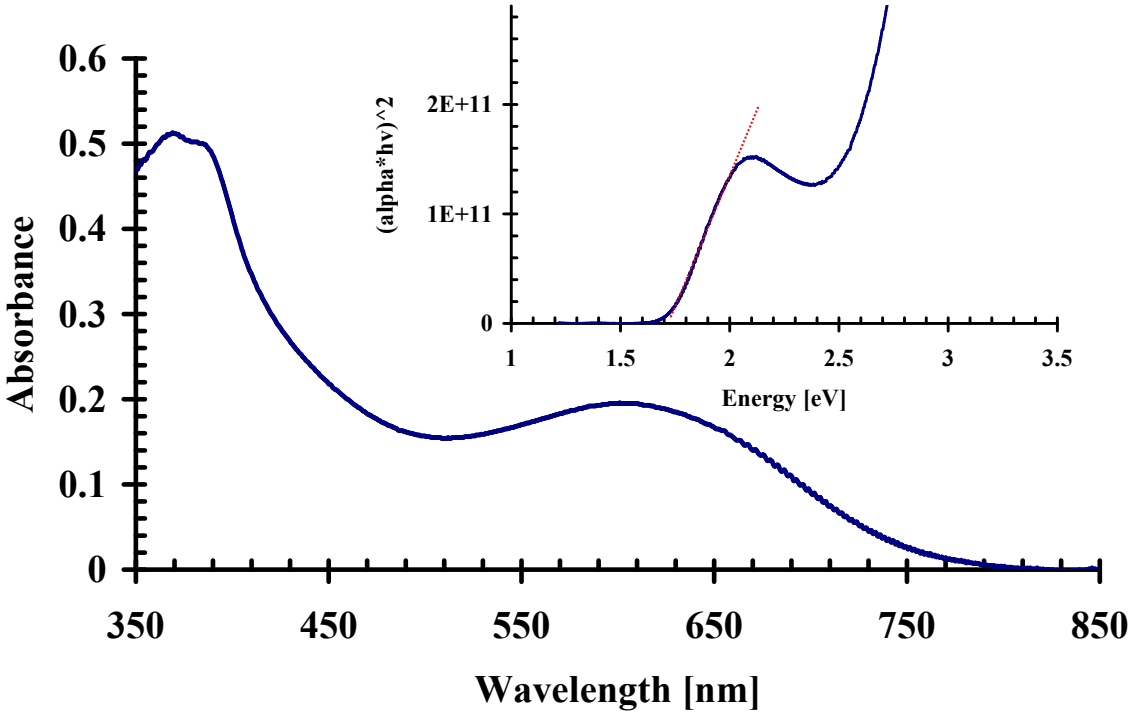

a)

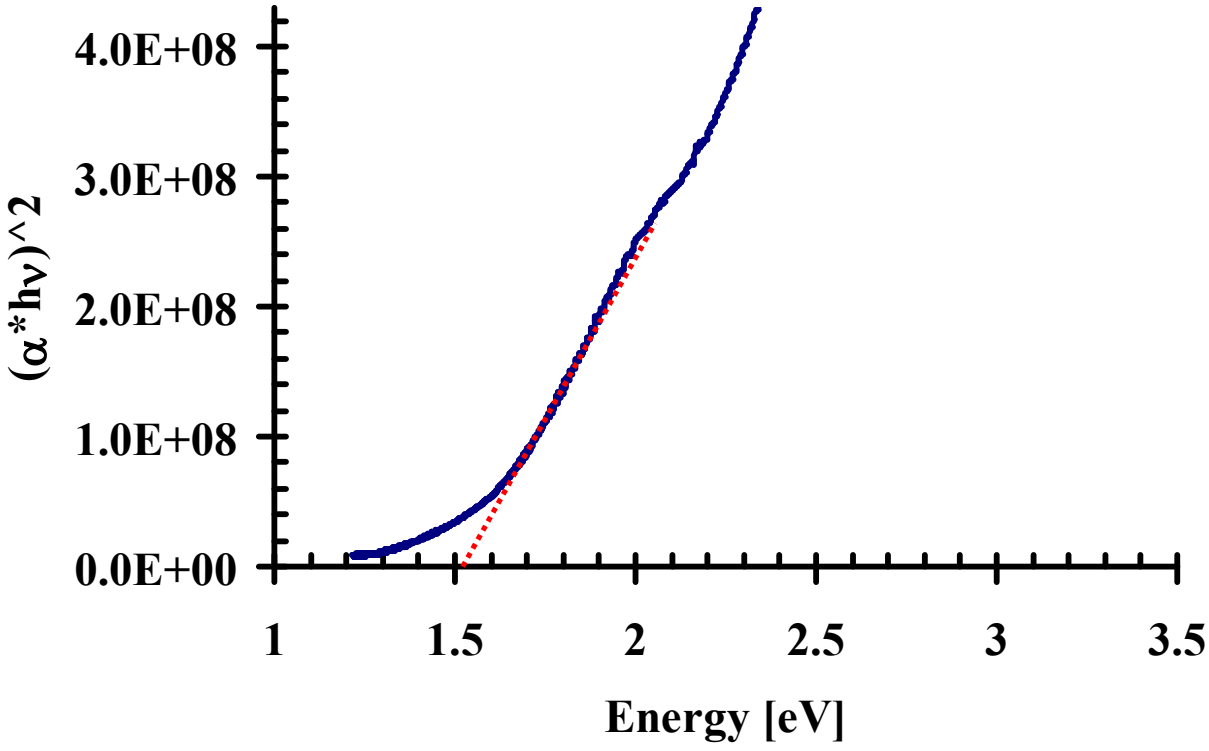

b)

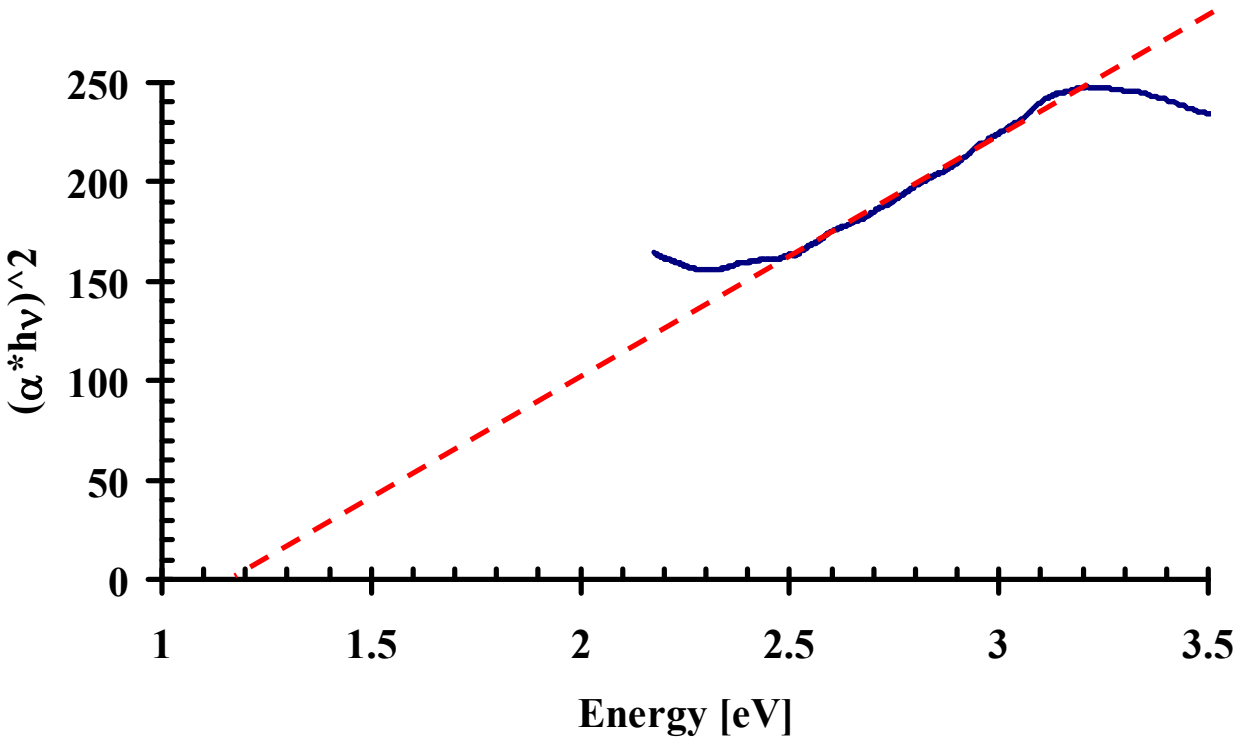

c)

Figure S7 – a) UV-Vis spectrum of PNDI2ODT4 thin film electrodeposited onto ITO/PET substrates. Inset: Spectrum elaboration according to eq.1 for n=1/2. **b)** Copol [1] band gap calculation; **c)** Copol [2] band gap calculation.

Band gap values of 1.5 eV and 1.15 eV have been calculated for Copol [1] and Copol [2] respectively.

7. Thin film morphology and solvent effects

Homopolymers and copolymers morphologies have been characterized by means of SEM and both the grain and the hole sizes distributions have been evaluated.

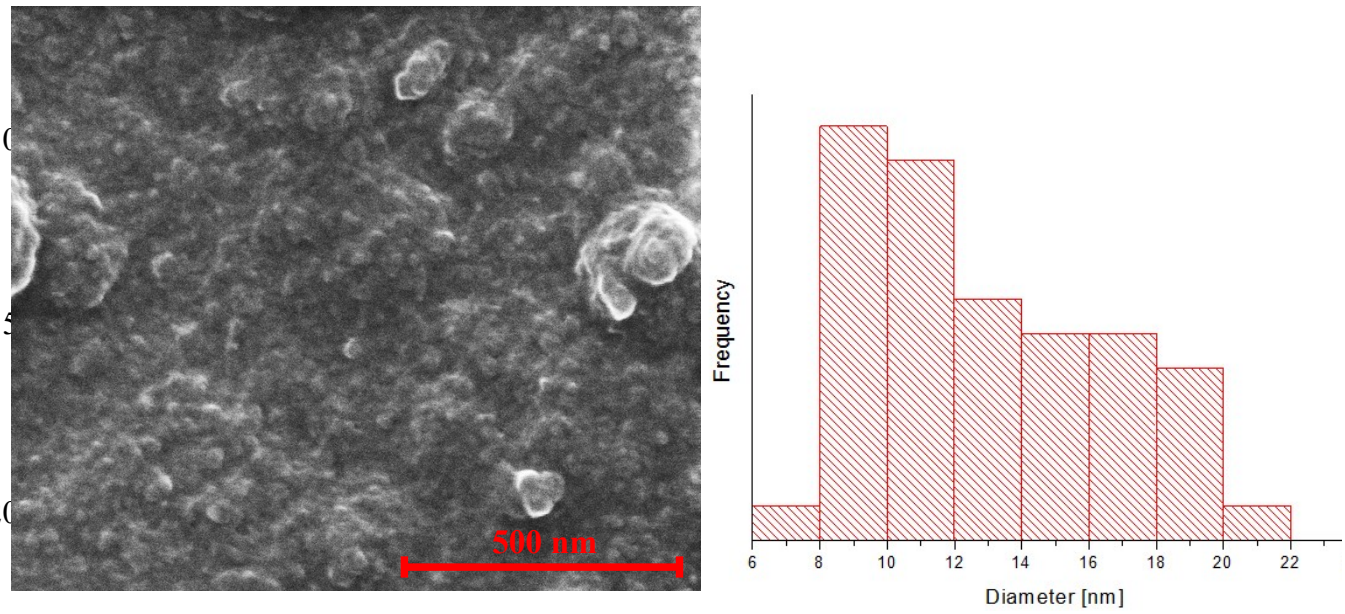

a)

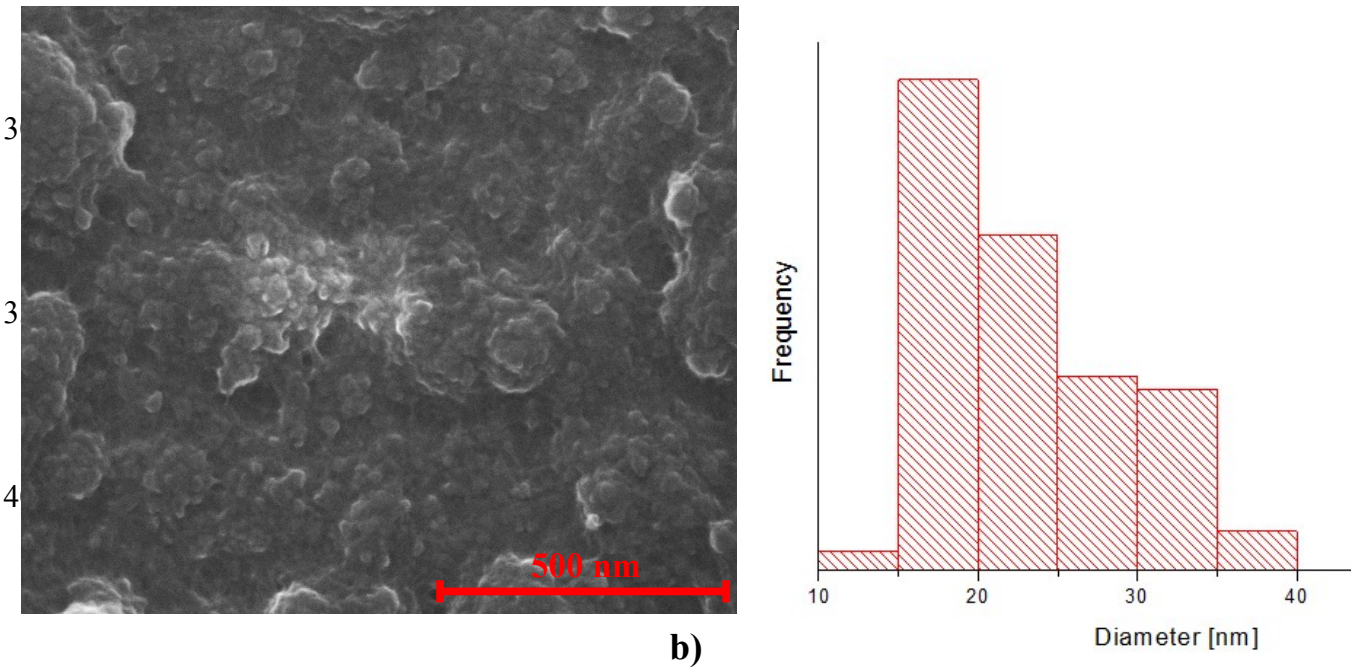

b)

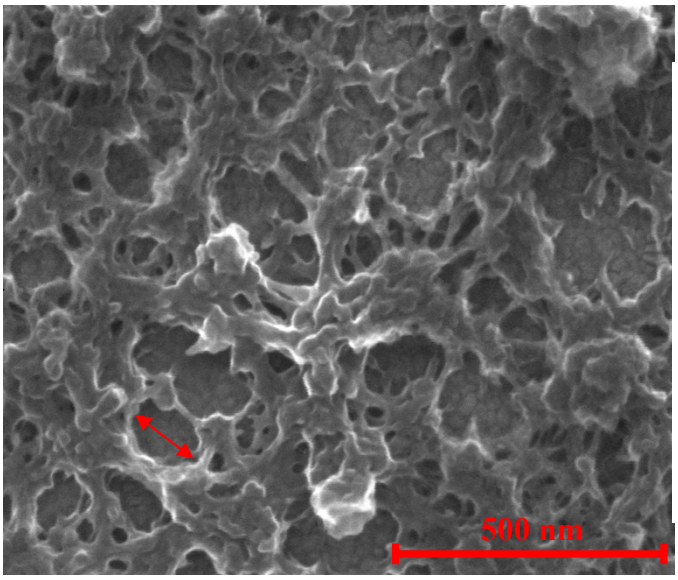
500 nm

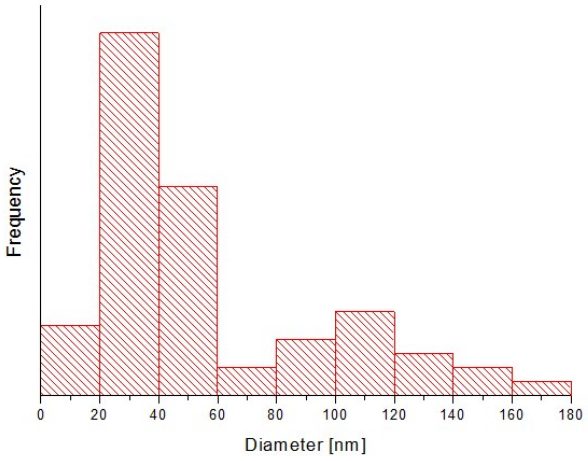
Frequency
0
20
40
60
80
100
120
140
160
180
Diameter [nm]

c)

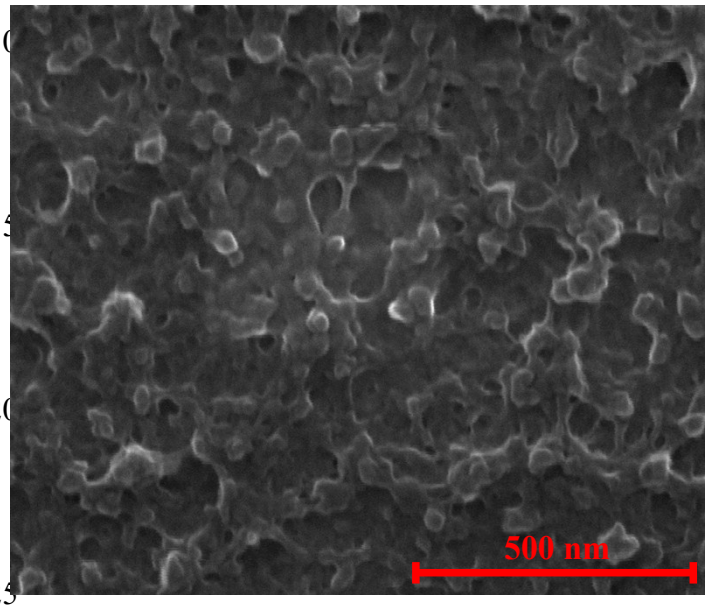
500 nm

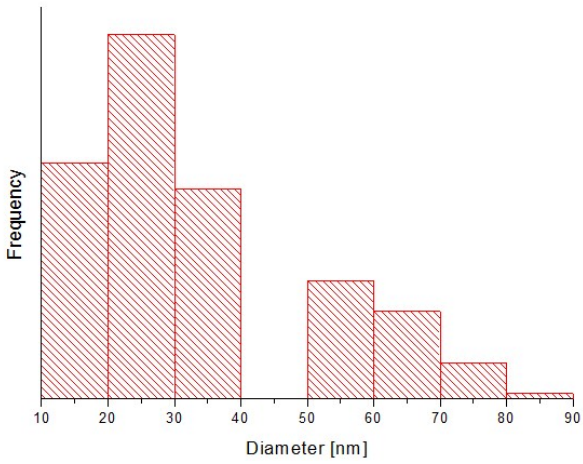
Frequency
10
20
30
40
50
60
70
80
90
Diameter [nm]

d)

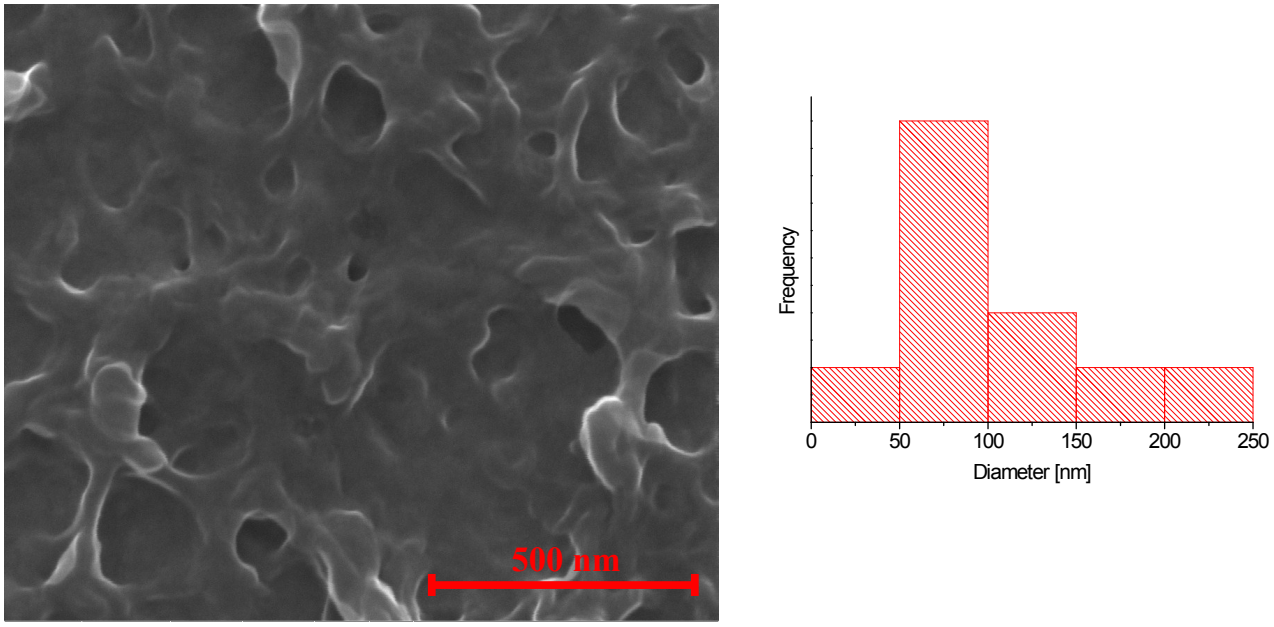

e)

Figure S8 – Thin film SEM images, grain and holes sizes distribution of: a) PNDI2ODT4; b) Copol [1]; c) Copol [2]; d) Copol [3]; e) PEDOT (Magnification: 100,000×).

Figure S8a displays PNDI2ODT4 surface. It appears as a compact layer with a particle grain size of 8–20 nm. Copol[1] displays a globular structure with particles 10-40 nm in size (see Figure S8b). EDOT rich polymers such as copol[2] show mainly porous features spanning between 10-180 nm as reported in Figure S8c. Copol[3] displays a less amount of porous features 15-100 nm together with globular nanoparticles 10-90 nm in size (see Figure S8d). PEDOT thin films show branched features with the presence of few pores with a diameter of 30-250 nm.

The double arrow line in fig.S8c indicates a typical pore with a diameter of about 130 nm. Statistical analysis has been performed by measuring the diameter of more than 100 pores for all the samples by the ImageJ software. All the thin films have not been metallized before the morphological analysis.

The choice of two solvents derives from the need of dissolving the monomer and obtaining a film with good adherence. CH_3CN does not dissolve NDI2ODT4 and CH_2Cl_2 furnishes very thin and not well adherent films. By mixing CH_2Cl_2 with a polar solvent (CH_3CN) we have obtained the best films as an indication that the increase of the solvent polarity promotes the polymer precipitation at the electrode surface. Figure S9 shows SEM images – performed with a FEI FEG-ESEM (mod. QUANTA 200) - of four PNDI2ODT4 metallized films obtained from

CH_2Cl_2:CH_3CN having different volume percentages. The magnification has been 100,000×. All the films display some crashes except the film electrodeposited in CH_2Cl_2:CH_3CN: (3:2; v:v) which appears homogeneous. This volume ratio has been chosen for all the experiments.

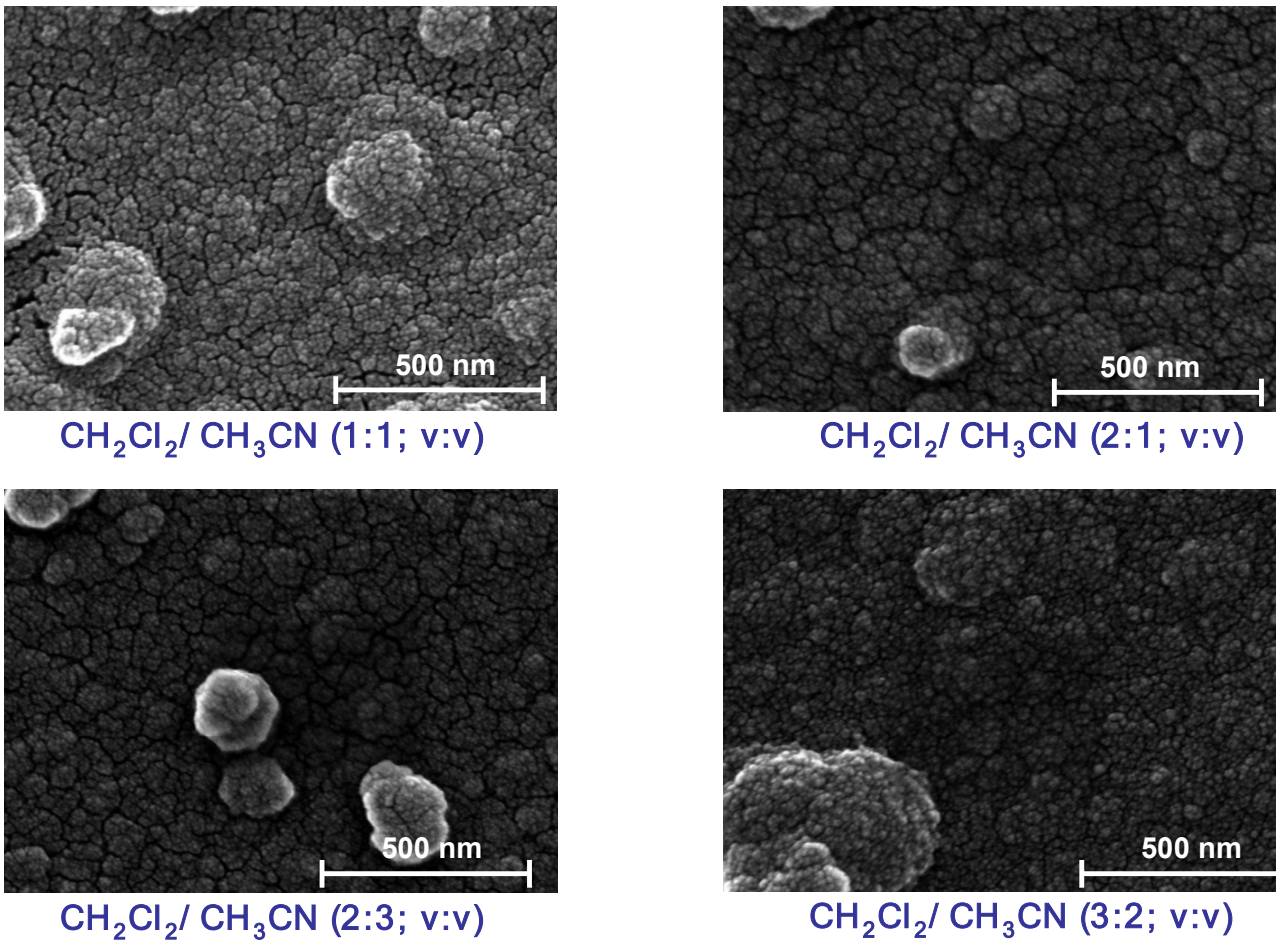

Figure S9a – SEM images of PNDI2ODT4 thin films deposited by CH2Cl2:CH3CN mixtures at different volume percentages (Magnification: 100,000×).

8. XPS of the Solid Supported Thin Films

Results of the XPS curve-fitting of C 1s photoelectron spectra of the electropolymerized thin films are reported in Table 2 and shown in Figure S10. The distribution of carbon species is expressed as peak area percentage (total C 1s peak area = 100%). Carbon peaks are assigned as follows: peak A (green peak) corresponds to C-C, C-H, C=C bonds; peak B (red peak) is attributed C-S, C-N bonds; peak C (cyan peak) to the presence of C-O bonds, peak D (olive peak) to N-C=O bonds. Peak E (purple) accounts for the asymmetric tail of the C 1s spectra, resulting from $\pi \rightarrow \pi^*$ shake up transition[7] and possibly positively polarized or charged carbon.[8]

Table 2. Results of the XPS curve-fitting of C 1s photoelectron spectra of the electropolymerized thin films. The distribution of carbon species is expressed as peak area percentage (total C 1s peak area = 100%).

SAMPLE	Peak A	Peak B	Peak C	Peak D	Peak E
BE (eV)	285.1	285.8	286.8	288.2	289.5
	C-H, C-C, C=C	C-S, C-N	C-O	N-C=O	Shake-up
PNDI2ODT4	80.0	14.6		5.4	
COPOL [1]	73.7	18.9		7.5	
COPOL [2]	38.9	29.3	21.3	10.5	
COPOL[3]	33.4	11.0	33.4	14.9	7.3
PEDOT	13.3	46.7	23.0	9.0	8.0

5

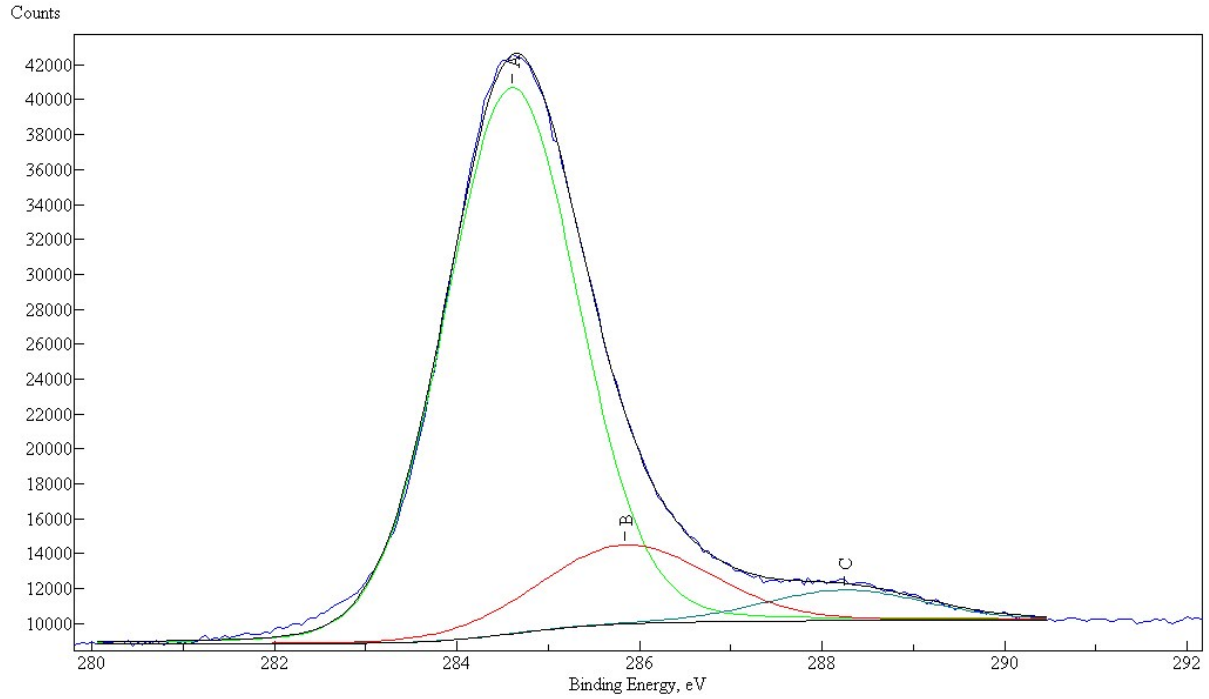
Counts
42000
40000
38000
36000
34000
32000
30000
28000
26000
24000
22000
20000
18000
16000
14000
12000
10000
A
B
C
280
282
284
286
288
290
292
Binding Energy, eV

a)

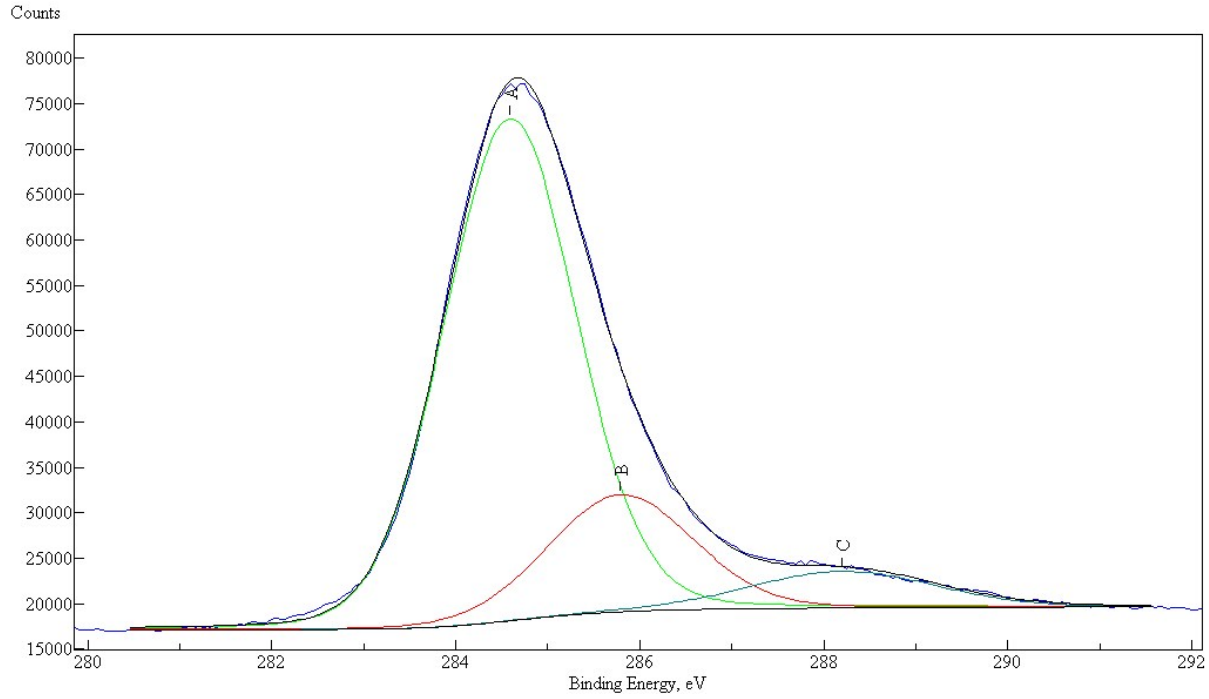
Counts
80000
75000
70000
65000
60000
55000
50000
45000
40000
35000
30000
25000
20000
15000
A
B
C
280
282
284
286
288
290
292
Binding Energy, eV

b)

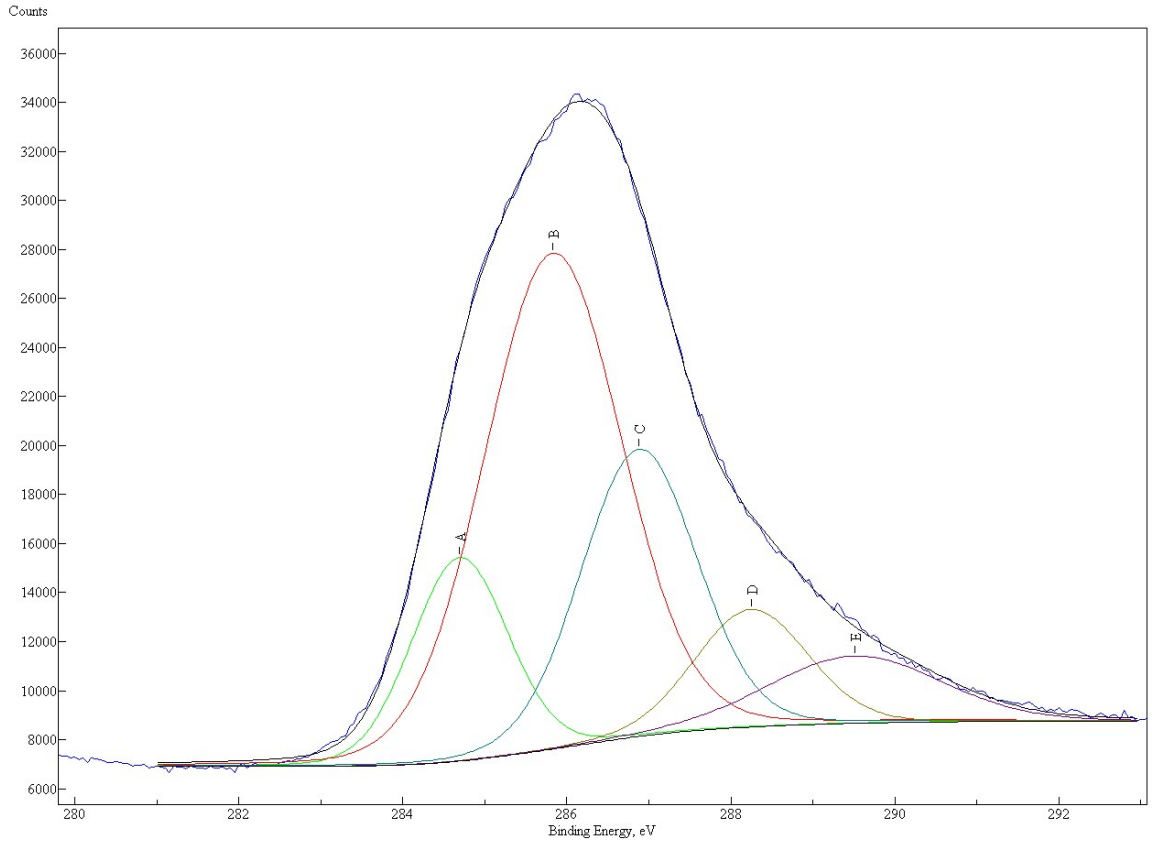
Counts
36000
34000
32000
30000
28000
26000
24000
22000
20000
18000
16000
14000
12000
10000
8000
6000
280
282
284
286
288
290
292
Binding Energy, eV
A
B
C
D
E

5 c)

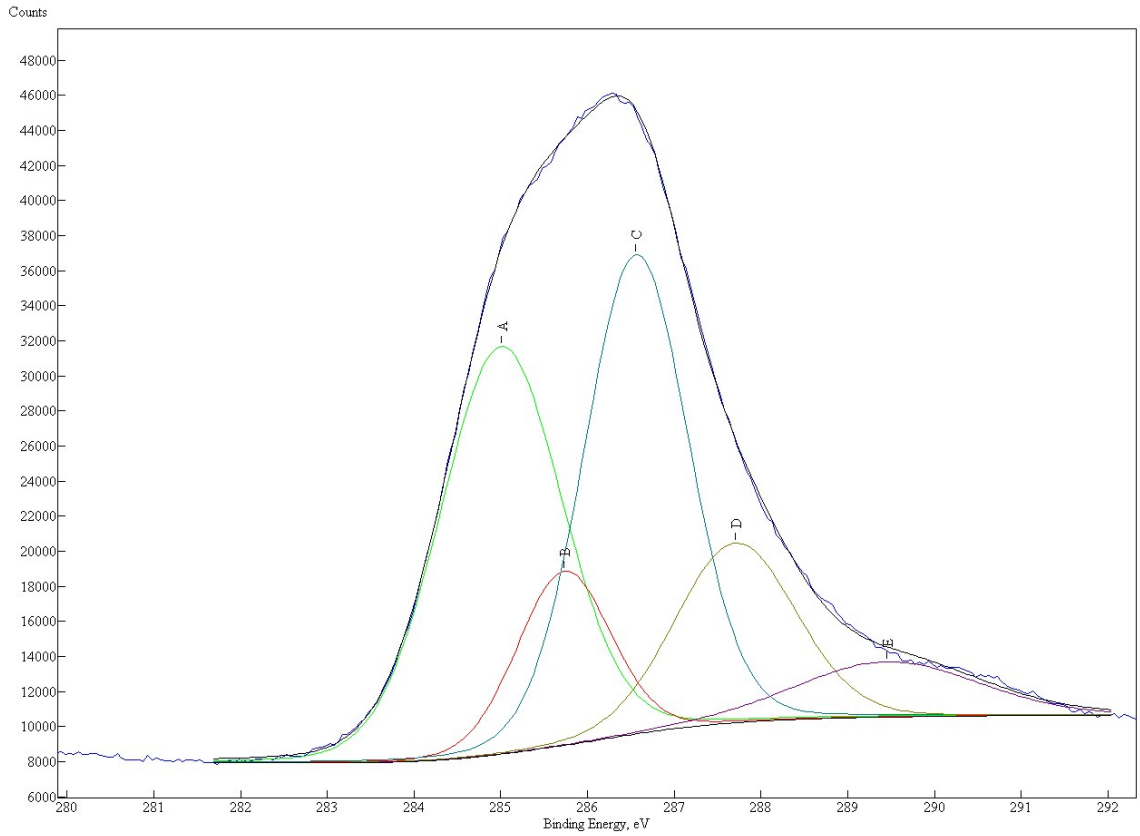

d)

Figure S10. XPS curve-fitting of the C 1s photoelectron spectra of the investigated thin film: a) PNDIT2ODT4; b) copol[1]; c) PEDOT; d) copol[3].

9. Electrical Measurements

The electrical measurements have been performed by a Keithley 4200-SCS Parameter Analyzer, configured in the voltage sweep mode. The metal contact with the organic thin layers electrodeposited on ITO/PET substrate was realized with circular orifices through Polytetrafluoroethylene (PTFE) substrate filled with mercury (Hg). The Hg contact area was 0.05 cm^2. The voltage has been maintained positive whereas the Hg potential was higher than that of ITO. Figure S11 shows the measured IV curves of the investigated structures in the -1.5-1.5 V bias range.

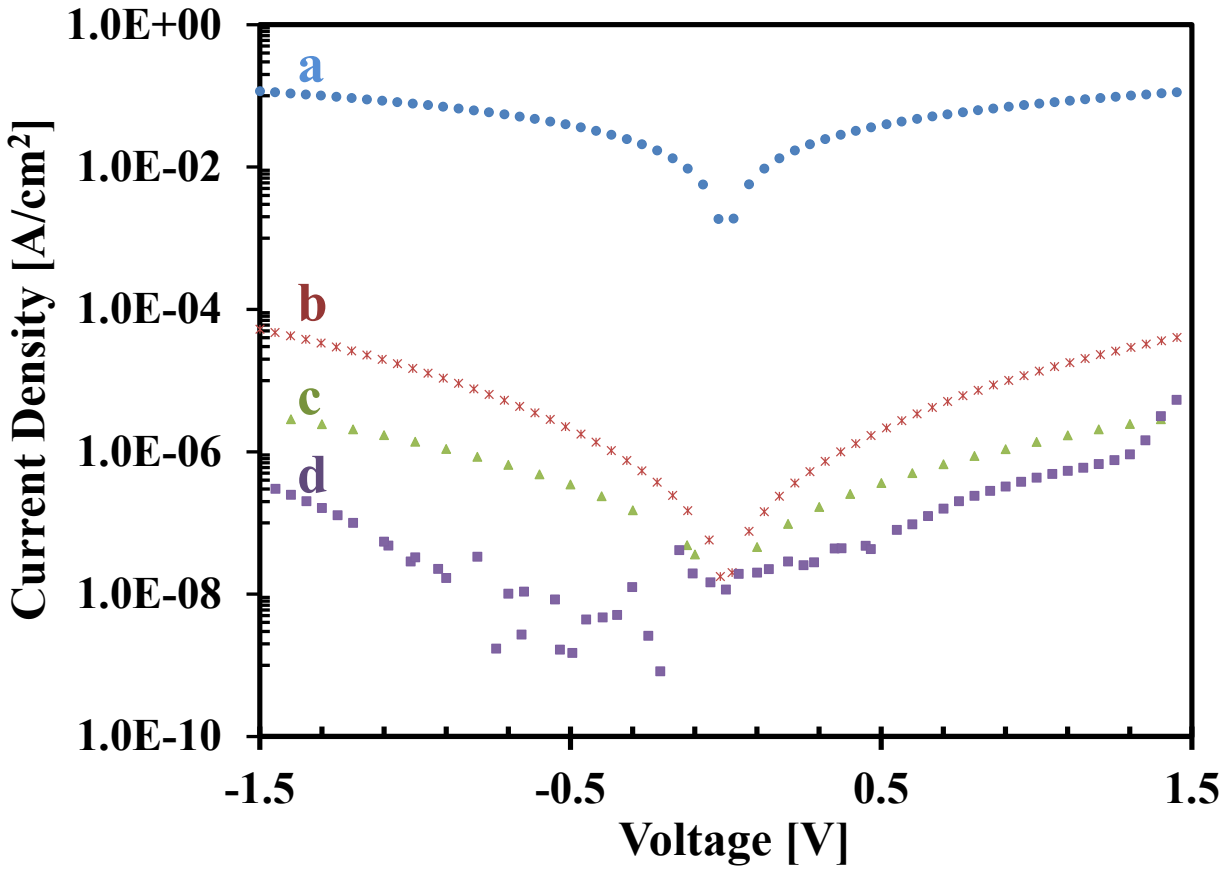

Figure S11 – Current density voltage curves: (a) PEDOT; (b) copol [2]; (c) copol [1] and (d) PNDI2ODT4.

10. Electrochromic Properties of PNDI2ODT4 Thin Films

The electro-optical properties of PNDI2ODT4 thin films have been investigated for understanding the changes in transmittance due to different redox states. For this reason, PNDI2ODT4 has been electrodeposited onto transparent ITO/PET electrodes (2.4 cm^2). The characterization has been led by employing 0.1 M $LiClO_4$ in CH_3CN and by using a two-electrodes configuration in a 1 cm cuvette endowed with quartz windows. For the estimation of the optical contrast, response time and coloration efficiency, we applied a potential square wave between +0.8V and -0.8V and the transmittance vs time curves have been recorded at 900 nm as shown in Figure S12.

The polymer displays an optical contrast of 19% and a high stability in the explored time and potential ranges. It appears green and light brown in the oxidised and reduced states, respectively. By considering the electrochemical charge required for a complete switching and the optical density at 900 nm, a coloration efficiency of 302 cm^2C^{-1} has been calculated. This value is comparable with the coloration efficiency of novel classes of poly(ether-imide)s [9].

PNDI2ODT4 exhibits slow response times compared to other poly(naphthalene)s derivatives [10].

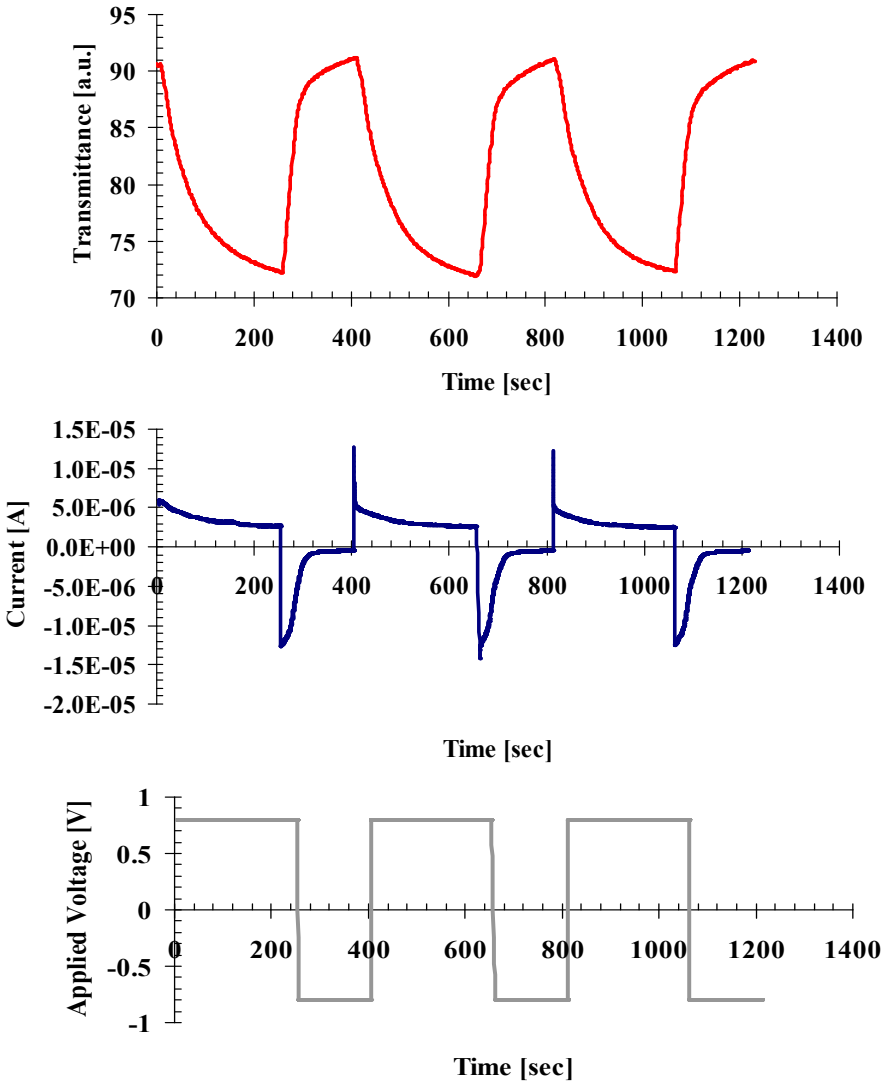

Figure S12 – Transmittance vs time (red plot) of a P NDI2ODT4 film under an applied potential square wave (grey plot) and the relative current transient (blue plot).

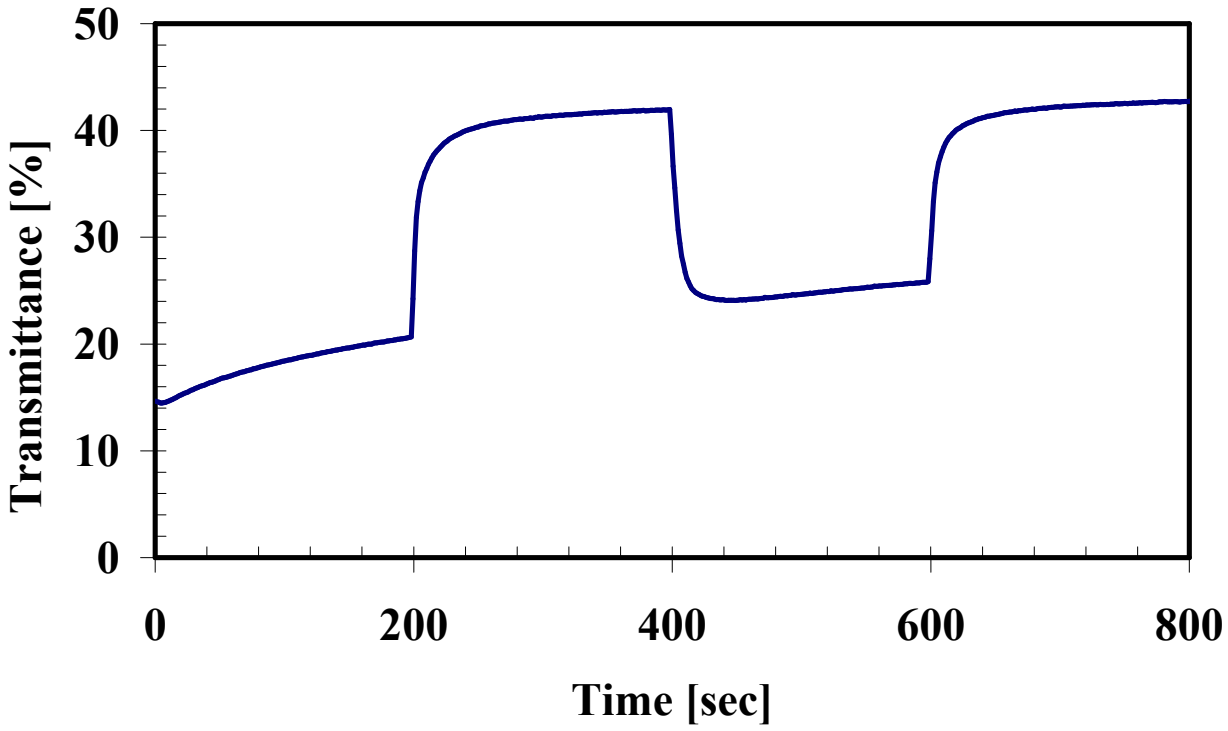

a)

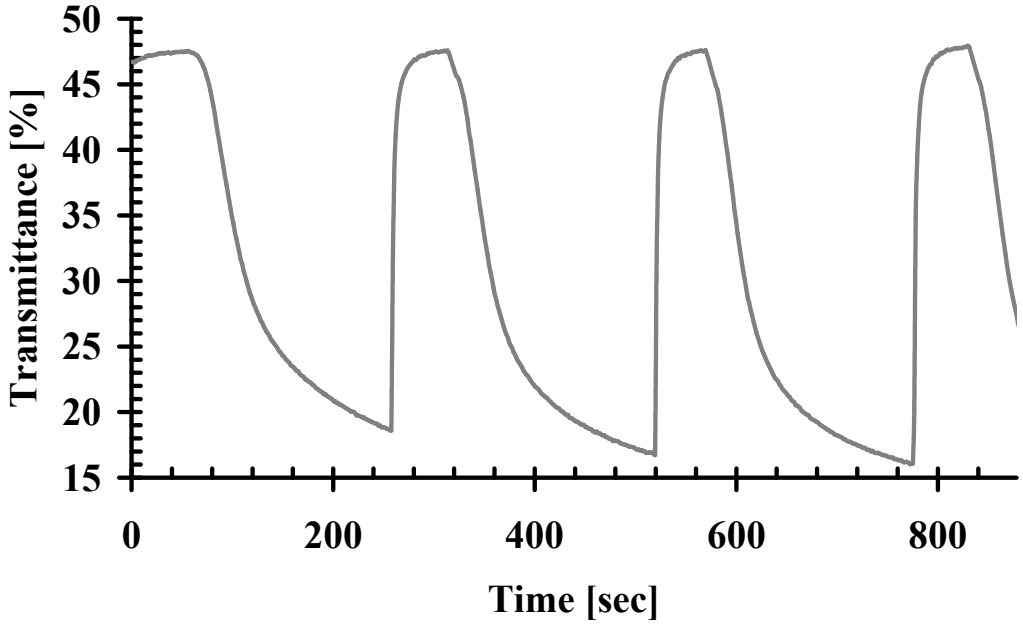

b)

Figure S13 – a) Transmittance vs time of Copol[1] film under an applied potential square wave between ±0.8 at 900 nm; **b)** Copol[3] based ECD spectroelectrochemical response.

Copol[1] (see Figure S13a) has exhibited the same optical contrast of PNDI2ODT4 at 900 nm and shorter response times but it has appeared unstable. Also, Copol[3] in ECD showed instability (see

transmittance variation in fig. S13b).

11. Contact angle measurements

Contact angle measurements have been performed by using a Contact Angle System DATAPHYSICS.

All the thin films have been wetted with a 10μL water drop. Table 3 summarizes the contact angle values of both homopolymers and copolymers thin films.

Table 3. Contact angles values

Film	Contact angle [deg]
PNDIT4	107.7
Copol [1]	118
Copol [2]	93.45
Copol [3]	65.35
PEDOT	45.1

12. Effect of monomer reduction

The electron affinity (E.A.) of the molecular models NDIT4-EDOT-NDIT4 (E.A. = 2.37 eV), NDIT4-$(EDOT)_4$-NDIT4 (E.A. = 2.32 eV), EDOT-NDIT4-EDOT (E.A. = 2.30 eV) and $(EDOT)_5$-NDIT4-$(EDOT)_5$ (E.A. = 2.26 eV) has been calculated by means of the ΔSCF approach, that is E.A. = $E_N - E_A$, where E_N and E_A are the SCF energies of the neutral molecule and the corresponding anion, respectively, whose geometries have been optimized at the CAM-B3LYP/cc-pVDZ level. Results show that an increase of EDOT content in an oligomer causes a small decreasing of the electron affinity. The tiny amount of this decreasing is attributable to a simple substituent effect of the EDOT chain, since the electron density associated with the additional electron in the anion species is almost exclusively localized in the NDIT4 moieties.

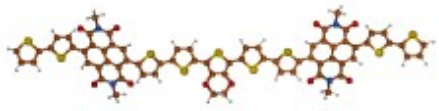

$N_1E_1N_1$ EA = 2.37 eV

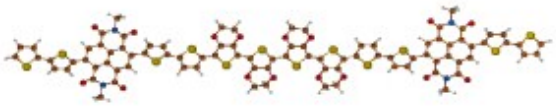

$N_1E_4N_1$ EA = 2.32 eV

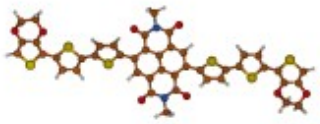

$E_1N_1E_1$ EA = 2.30 eV

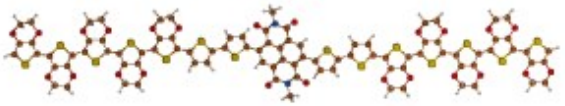

$E_5N_1E_5$ EA = 2.26 eV

13. Effect of thermal annealing on Copol [2] morphology

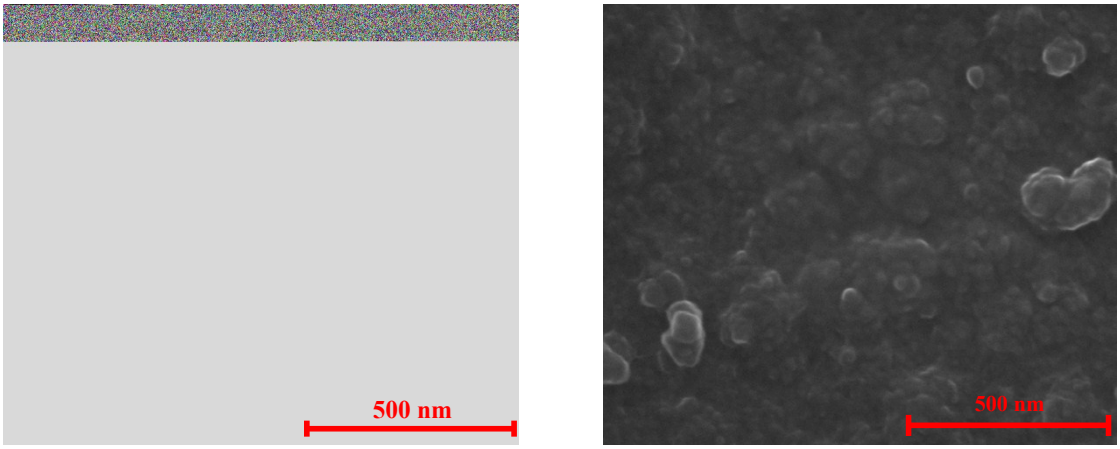

Fig. S14 Copol [2] morphology before (left) and after (right) the thermal annealing at about 160°C for 40 minutes

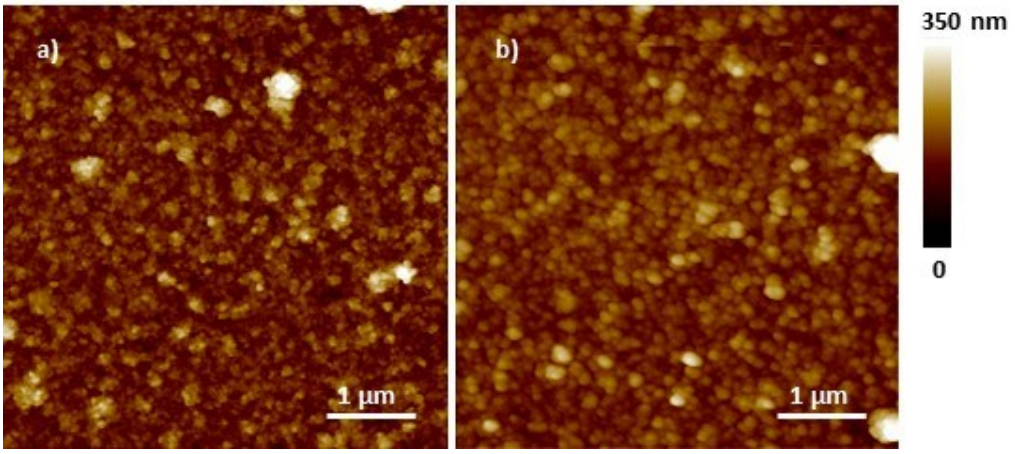

Figure S15: AFM morphology images of Copol2 samples before (a) and after (b) 40-minutes thermal annealing treatment at about 160°C.

Figure S9b shows AFM images of Copol2 sample surfaces as deposited and after undergoing the thermal annealing treatment. By measuring the mean surface roughness before and after the thermal treatment, it is worthy to note a decrease of about 20%, passing from 31.1 nm to 25.0 nm. Furthermore, the topography of both samples is characterised by spherical and amorphous aggregates. In the case of the non-annealed sample, the smaller aggregates have dimension spanning from 80 to 140 nm in diameter, while the bigger and massive aggregates are within the range 200 nm – 1 um. In the annealed sample, the smaller aggregates show dimensions of about 70-150 nm in diameter while the bigger ones are within 350 nm – 1.5 um.

14. References

[1] T. Yanai, D. Tew, N. Handy Chem. Phys. Lett., 393 (2004) 51.
[2] D. Jacquemin, V. Wathelet, E. A. Perpete, C. Adamo J. Chem. Theor. Comput. 5 (2009) 2420 ;
S. Kupfer, J. Guthmuller, L. González J. Chem. Theor. Comput. 9 (2013) 543.
[3] M. J. G. Peach, A. J. Cohen, D. J. Tozer Phys. Chem. Chem. Phys. 8 (2006) 4543.
[4] Gaussian 09, Revision C.01, M. J. Frisch, G. W. Trucks, H. B. Schlegel, G. E. Scuseria, M. A. Robb, J. R. Cheeseman, G. Scalmani, V. Barone, B. Mennucci, G. A. Petersson, H. Nakatsuji, M. Caricato, X. Li, H. P. Hratchian, A. F. Izmaylov, J. Bloino, G. Zheng, J. L. Sonnenberg, M. Hada, M. Ehara, K. Toyota, R. Fukuda, J. Hasegawa, M. Ishida, T. Nakajima, Y. Honda, O. Kitao, H. Nakai, T. Vreven, J. A. Montgomery, Jr., J. E. Peralta, F. Ogliaro, M. Bearpark, J. J. Heyd, E. Brothers, K. N. Kudin, V. N. Staroverov, R. Kobayashi, J. Normand, K. Raghavachari, A. Rendell, J. C. Burant, S. S. Iyengar, J. Tomasi, M. Cossi, N. Rega, J. M. Millam, M. Klene, J. E. Knox, J. B. Cross, V. Bakken, C. Adamo, J. Jaramillo, R. Gomperts, R. E. Stratmann, O. Yazyev, A. J. Austin, R. Cammi, C. Pomelli, J. W. Ochterski, R. L. Martin, K. Morokuma, V. G. Zakrzewski, G. A. Voth, P. Salvador, J. J. Dannenberg, S. Dapprich, A. D. Daniels, Ö. Farkas, J. B. Foresman, J. V. Ortiz, J. Cioslowski, and D. J. Fox, Gaussian, Inc., Wallingford CT, 2009.
[5] R.J. Waltman, J. Bargon, A.F. Diaz, J. Phys. Chem. 87 (1983) 1463.
[6] D.-K. Seo, R. Hoffmann Theor. Chem. Acc. 102 (1999) 23.
[7] a) Briggs, D. Surface analysis of polymers by XPS and static SIMS; Cambridge University Press: Cambridge, U.K.1998. b) Khan, M.A.; Armes, S.P.; Perruchot, C.; Ouamara, H.; Chehimi, M.M.; Greaves, S.T.; Watts, J.T. Langmuir 2000, 16, 4171; d) Jönsson, S.K.M.; Birgerson, J.; Crispin, X.; Greczynski, G.; Osikowicz, W.; Denier van der Gon, A.W.; Salaneck, W.R.; Fahlman, M. Synth. Met. 139 (2003) 1.
[8] a) Kang, E.T.; Neoh, K.G.; Tan, K.L. Phys. Rev. B: Condens. Matter Mater. Phys. 1991, 44, 10 461; b) Wu, C.R.; Nilsson, J.O.; Inganäs, O.; Salaneck, W.R.; Österholm, J.E.; Brédas, J.L.

Synth. Met. 21 (1987) 197.
[9] S. Hsiao, P. Chang, H. Wang, Y. Kung, T. Lee, Journal of Polymer Science, Part A: Polymer Chemistry 52 (2014) 825.
[10] J. Cai, L. Ma, H. Niu, P. Zhao, Y. Lian, W. Wang, Electrochimica Acta 112 (2013) 59.